

Bandwidth Efficient Digital Communication with Wavelet Approximations

Chet Lo and Todd K. Moon

Abstract: Based on their shift and scale orthogonality properties, scaling and wavelet functions may be used as signaling functions having good frequency localization as determined by the fractional-out-of-band power (FOOBP). In this paper, application of Daubechies' wavelet and scaling functions as baseband signaling functions is described, with a focus on finding discretely realizable pulse-shaping transfer function circuits whose outputs approximate scaling and wavelet functions when driven by more conventional digital signaling waveforms. It is also shown that the inter-symbol interference (ISI) introduced by the approximation has negligible effect on the performance in terms of signal-to-noise ratio (SNR). Moreover, the approximations are often more bandwidth efficient than the original wavelet functions. These waveforms thus illustrate an example solution of a tradeoff between residual ISI and bandwidth efficiency as a signal design problem.

Index Terms: Bandwidth efficient signaling, multiscale signaling, fractional out of bound power, wavelet.

I. INTRODUCTION

In recent years, an increasing number of applications of wavelet theory in various areas in digital communication have been established [1]–[3]. One of these approaches focuses on the study of wavelet functions themselves as the signaling functions [4]–[6]. Particularly, with their time-frequency localization properties, wavelet functions have good potential for providing bandwidth effective communication [7].

The spectral efficiency of a digital transmission system can be measured by the fractional-out-of-band power (FOOBP), which indicates as a function of bandwidth b what fraction of the total signal power lies outside the bandwidth b . Lower FOOBP indicates superior bandwidth efficiency. Following Ziemer's convention [8], the FOOBP can be computed by the following definition $FOOBP(b) = 1 - \frac{2}{P_T} \int_0^{\frac{b}{2}} G(f)df$, where b is the bandwidth, $G(f)$ is the power spectral density of the signal of interest, and P_T is the total power of the signal. Quadrature signaling is used for all the signaling functions in this paper.

Daubechies' wavelets are orthogonal with respect to integer shifts, which means that several overlapping Daubechies' wavelets can be used to carry information through the same physical channel [9]. The shift orthogonality allows them to be inter-symbol interference (ISI)-free at the output of an appropriately designed matched filter on the receiving end.

As Fig. 1 demonstrates [6], compared to other traditional signaling functions employed in digital communication, wavelet

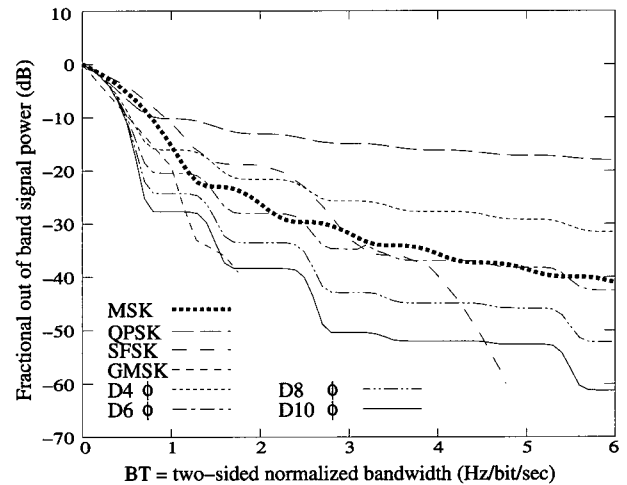


Fig. 1. Comparison of the FOOBP for MSK, QPSK, SFSK, GMSK, ϕ_4 , ϕ_6 , ϕ_8 , and ϕ_{10} .

signaling has significantly better bandwidth efficiency. Fig. 1 shows the comparison of the FOOBP for various scaling functions of D_4 , D_6 , and D_8 , which are Daubechies' families of wavelet with difference number of coefficients, with that for QPSK (square wave), SFSK, GMSK, and MSK. Even setting aside other potential benefits of wavelets, the bandwidth efficiency of wavelet signaling makes it worth studying.

Because of the bandwidth efficiency of wavelet signaling, we are motivated to examine means of producing with special circuitry to shape a time pulse to closely approximate the desirable characteristics of wavelet waveforms. In particular, we examine pulse shaping circuits which produce pulses having good spectral efficiency and shift orthogonality. The resulting shaped waveforms do not have perfect shift orthogonality, so some minor ISI is introduced. However, as we show, the probability of error performance is only negligibly affected.

This paper begins by studying the basic structure and frequency domain properties of high-dimension composite signals in Section II. Then in Section III, we study the method for finding the rational transfer functions for pulse shaping. The penalty introduced by the residue ISI is studied and presented in Section IV. In Section V, we present FOOBP for examples from Daubechies' wavelet approximations compare with that of original wavelet functions. Section VI presents conclusions and discussions.

II. HIGH-DIMENSION COMPOSITE SIGNALS

In Daubechies' construction of wavelets, there are two basic functions: The wavelet function, ψ , and the scaling function, ϕ .

Manuscript received February 6, 2001; approved for publication by Dong In Kim, Division II Editor, August 15, 2001.

The authors are with Electrical and Computer Engineering Department, Utah State University, Logan, UT 84322, e-mail: chetlo@cc.usu.edu.

As scaling functions are orthogonal to wavelet functions on its scale or shorter scales, and wavelet functions on different scales are orthogonal to each other. So, we may transmit information using high-dimension composite signals constructed, in such a way that wavelets on each scale do not interfere with wavelets on other scales. For example, we can have composite signal $U(t)$ with $N + 1$ scales, such that a single "frame" of the signal can be represented as

$$U(t) = E_b \left\{ a_\phi 2^{-N/2} \phi(2^{-N}t) + \sum_{j=1}^N \sum_{l=0}^{2^{(N-j)}-1} a_{\psi,j,l} 2^{-j/2} \psi(2^{-j}t - l) \right\}, \quad (1)$$

where E_b is the energy per bit, and $a_\phi, a_{\psi,j,l} \in \{-1, 1\}$ are the information bits that are carried with a scaling function ϕ and by wavelet functions on scale j , respectively. To facilitate our following discussion, it will be convenient to introduce more compact notation. Using

$$\gamma_k(t) = \begin{cases} 2^{-N/2} \phi(2^{-N}t) & k = 0 \\ 2^{-j/2} \psi(2^{-j}t - l) & k = 2^{(N-j)} + l, j = 1, \dots, N, \\ & \text{and } l = 0, \dots, 2^{(N-j)} - 1, \end{cases} \quad (2)$$

and

$$b_k = \begin{cases} a_\phi & k = 0 \\ a_{\psi,j,l} & k = 2^{(N-j)} + l, j = 1, \dots, N, \\ & \text{and } l = 0, \dots, 2^{(N-j)} - 1, \end{cases} \quad (3)$$

to represent the wavelets and their information carrying-bits on the different scales, we can rewrite (1) as

$$U(t) = E_b \sum_{k=0}^{2^N} b_k \gamma_k(t). \quad (4)$$

According to Daubechies [9], we know that $|\hat{\phi}(2\omega)|^2 + |\hat{\psi}(2\omega)|^2 = |\hat{\phi}(\omega)|^2$. So, the power spectrum of the high-dimension signal can be expressed as $|\hat{\phi}(2^N\omega)|^2 + \sum_{j=1}^N |\hat{\psi}(2^j\omega)|^2 = |\hat{\phi}(\omega)|^2$. That is, this composite signal has the same spectral performance as $\phi(t)$. Theoretically, we cannot achieve spectral performance that is superior to single scaled scaling functions by using high-dimension composite signals. However, as will be shown in the following, due to imperfect rational approximation, composite signal approximations can give us superior bandwidth performance.

III. FREQUENCY DOMAIN APPROXIMATIONS OF SCALING AND WAVELET FUNCTIONS

We now consider the problem of finding circuits with rational transfer functions whose output approximates a wavelet function or a scaling function when driven by some given input functions. We call these input functions stimulating functions. That is, we want to find the transfer functions of circuits whose responses to some stimulating function $S_{\phi_N}(s)$ and $S_{\psi_N}(s)$ are the corresponding approximations of scaling function and wavelet function, respectively, i.e.,

$$\Phi_N(s) \approx H_{\phi_N}(s) S_{\phi_N}(s), \quad (5)$$

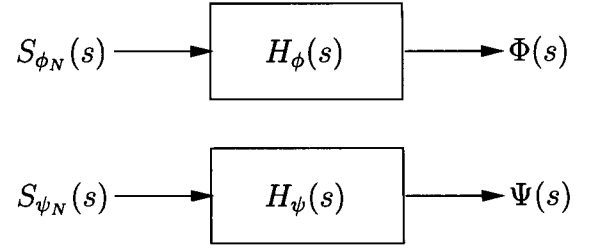


Fig. 2. The illustration of analog circuit framework to produce (approximate) scaling function and wavelet function.

Table 1. List of scaling function and wavelet functions, and execution parameter.

| Func. number | execution parameter | | | | | | stimulating func. |
|--------------|---------------------|-----|----------|---------|-----|-----|-------------------|
| | approximating | P | α | β | q | p | |
| S1 | $\phi_4(t)$ | 50 | -3 | 3 | 2 | 3 | unit pulse |
| S2 | $\phi_6(t)$ | 50 | -3 | 3 | 2 | 5 | unit pulse |
| S3 | $\phi_8(t)$ | 50 | -3 | 3 | 5 | 8 | unit pulse |
| S4 | $\phi_{10}(t)$ | 50 | -3 | 3 | 4 | 7 | unit pulse |
| S5 | $\phi_6(t/2)$ | 50 | -2.5 | 2.5 | 4 | 8 | unit sine pulse |
| W1 | $\psi_6(t/2)$ | 50 | -2.5 | 2.5 | 6 | 9 | double sine pulse |

and

$$\Psi_N(s) \approx H_{\psi_N}(s) S_{\psi_N}(s), \quad (6)$$

where $\Phi(s)$ is the Laplace transform of $\phi(t)$, $\Psi(s)$ is the Laplace transform of $\psi(t)$, and $H_{\phi_N}(s)$ is the transfer function for the circuit that generates a scaling function, while $H_{\psi_N}(s)$ is for the circuit that generates a wavelet function. This concept is illustrated in Fig. 2. We employ the Second Algorithm of Remes [10], [11] (Chebyshev approximation) to generate the rational approximations.

Since wavelets are causal, we can convert the Fourier transform of the scaling function and the wavelet function to their Laplace transforms, that is

$$\Phi_N(s) = M_0\left(\frac{s}{2}\right) M_0\left(\frac{s}{4}\right) \cdots M_0\left(\frac{s}{2^j}\right) \cdots, \quad (7)$$

$$\Psi_N(s) = \frac{1}{2} \sum_{n=0}^{2^N-1} c_{N-1-n} (-1)^n e^{-\frac{ns}{2}} \Phi_N\left(\frac{s}{2}\right), \quad (8)$$

and

$$M_0(s) = \frac{1}{2} \sum_{n=0}^{2^N-1} c_n e^{-ns}. \quad (9)$$

where $\{c_n\}$ are coefficients for different Daubechies' wavelet families [9]. Moreover, as wavelet are analytic [6], the approximation can be done along the real axis. We will set the region of approximation to be (α, β) . Let

$$H_{qp}(s) = \frac{b_q s^q + b_{q-1} s^{q-1} + \cdots + b_0}{a_p s^p + a_{p-1} s^{p-1} + \cdots + a_1 s + 1} \approx F(s) \quad \text{for } \alpha \leq s \leq \beta, \quad (10)$$

where $H_{qp}(s)$, our desired approximation, has numerator polynomial of degree at most q and denominator polynomial of de-

Table 2. Rational Chebyshev approximation of scaling and wavelet functions.

| | |
|--|---|
| $H(s) = \frac{b_q s^q + b_{q-1} s^{q-1} + \dots + b_0}{a_p s^p + a_{p-1} s^{p-1} + \dots + a_0}$ <p style="text-align: center;">num: b_q, b_{q-1}, \dots, b_0</p> <p style="text-align: center;">den: a_p, a_{p-1}, \dots, a_0</p> | |
| S1 ($p = 3, q = 2$) | num: 6.07965E-2, 5.50072E-1, 1.02714 den: 1.80884E-2, 1.77583E-1, 6.70270E-1, 1.00000 |
| S2 ($p = 5, q = 2$) | num: 1.73485E-1, 7.67364E-1, 1.03427 den: 4.85543E-4, 1.39702E-2, 1.20040E-1, 4.91232E-1, 1.05618, 1.00000 |
| S3 ($p = 8, q = 5$) | num: 2.50635E-3, 1.05982E-2, 8.33368E-2, 4.32409E-1, 1.05086, 9.92191E-1 den: 1.67269E-5, 3.98844E-4, 4.50141E-3, 3.16942E-2, 1.52276E-1, 5.08033E-1, 1.14038, 1.56449, 1.00000 |
| S4 ($p = 7, q = 4$) | num: 6.33948E-3, 2.53829E-2, 2.29281E-1, 8.61608E-1, 9.78576E-1 den: 2.13333E-4, 3.98380E-3, 3.21716E-2, 1.54005E-1, 5.00442E-1, 1.12691, 1.57462, 1.00000 |
| S5 ($p = 8, q = 4$) | num: 8.69278E-3, 2.70141E-2, 2.59978E-1, 1.10364, 1.57048 den: 2.76342E-7, -4.89612E-6, -3.04270E-5, 1.06794E-3, 1.69826E-2, 1.17846E-1, 4.62641E-1, 1.02014, 1.00000 |
| W1 ($p = 9, q = 6$) | num: -1.69629E-4, 1.80456E-3, -1.97358E-2, 7.61421E-2, -3.12574E-1, 9.51355E-10, 1.88255E-11 den: 2.63115E-7, 8.38887E-6, 1.35269E-4, 1.43198E-3, 1.08072E-2, 5.96765E-2, 2.39356E-1, 6.69234E-1, 1.18115, 1.00000 |

gree at most p . The function $F(s)$ to be approximated is either

$$F(s) = \frac{1}{S_{\phi_N}(s)} \prod_{k=1}^P M_0\left(\frac{s}{2^k}\right), \quad (11)$$

for the scaling function, or

$$F(s) = \frac{1}{2S_{\psi_N}(s)} \sum_{n=0}^{2N-1} c_{N-1-n} (-1)^n e^{-\frac{ns}{2}} \prod_{k=1}^P M_0\left(\frac{s}{2^{k+1}}\right), \quad (12)$$

for the wavelet function. P is an approximation design parameter, the number of terms we retain in the infinite product of $M_0(\cdot)$. Let

$$r_{qp}(s) = H_{qp}(s) - F(s), \quad (13)$$

and

$$r_{qp} = \max_{\alpha \leq s \leq \beta} |r_{qp}(s)|. \quad (14)$$

The minimax solution is the choice of b 's and a 's that minimizes r_{qp} . Then, b_q, b_{q-1}, \dots, b_0 and a_p, a_{p-1}, \dots, a_1 are the coefficients we desire.

Due to the properties of the wavelet function and scaling function, we pick a lowpass signal as the stimulating function for the lowpass scaling function, and a bandpass signal as the stimulating function for the bandpass wavelet function.

We consider two sets of designs. In the first set, only the scaling function is employed as signaling pulse. We use

$$S_{\phi_N}(s) = \frac{1 - e^{-s}}{s}, \quad (15)$$

which is the Laplace transform of unit pulse function $s_{\phi_N}(t) = u(t) - u(t-1)$, as the stimulation function. In the second set, we consider the high-dimension composite signal. Here, we use

$$S_{\phi_N}(s) = \frac{\pi(1 + e^{-s})}{s^2 + \pi^2}, \quad (16)$$

the Laplace transform of unit sine pulse function $s_{\phi_N}(t) = \sin(\pi t)$ for $0 \leq t \leq 1$, as the stimulation function for the scaling function. For the wavelet function we use

$$S_{\psi_N}(s) = \frac{\frac{1}{2}\pi(1 - e^{-s})}{\frac{1}{4}s^2 + \pi^2}, \quad (17)$$

the Laplace transform of double sine pulse function $s_{\psi_N}(t) = \sin(2\pi t)$ for $0 \leq t \leq 1$, as the stimulating function.

Because (7) and (8) are infinite-order systems, any finite-order approximation must sacrifice some of the attributes of the original function. In our investigations, we examined many approximations using different orders of filters and approximation ranges, and present here only those which best preserve the orthogonality properties.

The transfer functions are numbered and their approximation parameters are listed in Table 1. **S1** to **S4** are the examples for the scaling function approximations from the first set of experiments we mention above. **S5** and **W1** are the example of the function pair from the second set of experiments for high-dimension composite signal.

The main results for this paper are shown in Table 2. The numbering used in Table 1 appears in small boxes on the top left corner for each row, with the value of p and q indicating the order of numerator terms and denominator terms, respectively.

IV. ERROR AT INTEGER SHIFTS

On the receiver side of the communication system, a matched filter bank is used to detect the transmitted signal. Let us consider the response of the matched filter $\gamma_s(t)$ to the signal $U(t)$

Table 3. Δ_{dB} and correlations for wavelet approximations.

| # | Δ_{dB} (dB) | Correlation | | | | | | | |
|----|--------------------|-------------|-------------|-------------|-------------|-------------|-------------|----------|--|
| S1 | 2.01181E-2 | 4.15619E-2 | -1.47214E-2 | 7.16069E-4 | 6.36922E-5 | 8.12059E-5 | 8.77103E-5 | R_{S1} | |
| S2 | 4.22966E-2 | 5.74400E-2 | -2.82503E-2 | 5.98278E-3 | -1.88594E-4 | 3.59533E-5 | 9.78387E-5 | R_{S2} | |
| S3 | 1.66980E-3 | -1.13414E-2 | 5.02764E-3 | -1.96735E-3 | 7.03149E-4 | -1.34030E-5 | 5.79867E-5 | R_{S3} | |
| S4 | 2.41648E-2 | -3.88732E-2 | 2.61170E-2 | -1.01236E-2 | 9.02724E-4 | 2.42000E-3 | -2.80755E-3 | R_{S4} | |
| S5 | 1.71747E-2 | 6.60758E-3 | -3.42569E-3 | 9.64710E-4 | 1.54898E-4 | 6.69687E-5 | 8.07632E-5 | R_{S5} | |
| W1 | 1.89750E-2 | 2.08889E-3 | 1.46137E-2 | 2.30932E-3 | 2.24934E-3 | 2.58523E-4 | -9.28162E-5 | * | |
| | | | | | 2.98886E-4 | 6.56378E-5 | 1.13203E-5 | R_{W1} | |

Note: * is shared between R_{S5} and R_{W1} .

given in (4),

$$d_{\gamma_s} = \int U(t)\gamma_s(t)dt$$

$$= E_b \left\{ \sum_{k \neq s} \int b_k \gamma_k(t) \gamma_s(t) dt + \int b_s \gamma_s(t) \gamma_s(t) dt \right\}. \quad (18)$$

Let

$$R_{\gamma_s, \{b_k\}} = E_b \sum_{k \neq s} \int b_k \gamma_k(t) \gamma_s(t) dt \quad (19)$$

be the sum of the correlations involving $\gamma_s(t)$ and the other wavelets in the frame of $U(t)$. The subscript $\{b_k\}$ of $R_{\gamma_s, \{b_k\}}$ indicates that its value depends on the different combination of b_k 's. When all the functions in $U(t)$ are shift- and scale-orthogonal among themselves, we have $R_{\gamma_s, \{b_k\}} = 0$ for all γ_s , and the signal is ISI-free.

The rational approximations of the transfer functions we have presented preclude exact realization of the shift- and scale-orthogonality properties. Therefore, correlation of the successively generated signals introduces ISI at the receiver. Without loss of generality, we may assume $b_s = 1$. Then, to calculate the probability of error with the presence of ISI, we consider all the 2^{2^N-1} possible combinations of ± 1 's the b_k can be for each of $R_{\gamma_s, \{b_k\}}$. We call the set of these possible combinations $\{b_k\}$ as \mathcal{B} . By assuming that the probabilities of the occurrence of different $\{b_k\}$ being equal, the probability of error with the presence of ISI can be derived as follows. If the transmitted bit energy is E_b , then the received bit energy for function $\gamma_s(t)$ is $E_b(1 + R_{\gamma_s, \{b_k\}})$ and the probability of error is

$$P_{\gamma_s}(\{b_k\}) = Q \left(\sqrt{\frac{2E_b(1 + R_{\gamma_s, \{b_k\}})}{N_0}} \right), \quad (20)$$

where N_0 is the noise level. When we sum over all 2^{2^N-1} possible combinations in \mathcal{B} , we have the probability of error with the presence of ISI, which is given by

$$P_{\gamma_s}(ISI) = \frac{1}{2^{2^N-1}} \sum_{\{b_k\} \in \mathcal{B}} P_{\gamma_s}(\{b_k\}). \quad (21)$$

The overall probability of error can be obtained by averaging the above value over all $\gamma_s(t)$,

$$P_b(ISI) = \frac{1}{2^{2^N}} \sum_{\gamma_s} P_{\gamma_s}(ISI). \quad (22)$$

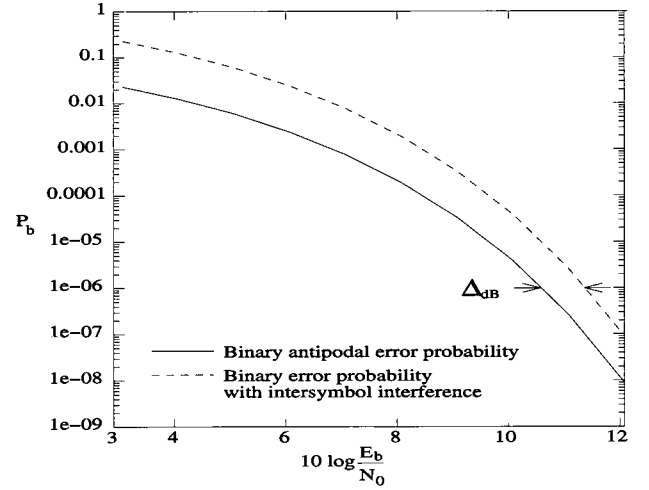


Fig. 3. Correlation penalty in probability of error performance due to ISI. The penalty is greatly expanded from results actually obtained for the purpose of illustration.

A system with ISI requires a higher signal-to-noise-ratio (SNR) than a system without ISI to achieve an equal probability of error. This difference in SNR is defined as correlation penalty. Fig. 3 illustrates the effect of correlation on the probability of error (the difference is exaggerated from results actually obtained for illustration). The correlation penalty at an error of $P_b = 10^{-6}$ is designated as Δ_{dB} , as shown in the figure. A list of corresponding correlation penalties for those transfer functions we numbered above can be found in Table 3. We find that the correlation penalty we have to pay for using wavelet approximations is very small, in all cases less than 0.05 dB.

V. FOOBP OF THE APPROXIMATIONS

While the rational approximations slightly decreases the SNR performance of the signaling, in general we gain in the FOOBP performance. We plot the FOOBP of those transfer functions numbered above along with the FOOBP of the theoretical scaling functions in Figs. 4 and 5. From the plots, we can see that transfer functions have FOOBP even superior to these original scaling functions that are being approximated. Fig. 4 presents FOOBP of scaling functions and their single scale approximations. We observe that the approximations to the scaling functions roll off faster than the exact scaling functions. As bandwidth increases, rational functions, with smoother time response than wavelets, have lower FOOBP than wavelets.

When we are using composite high-dimensional signals, the bandwidth performance can be even better. In Table 1, we have

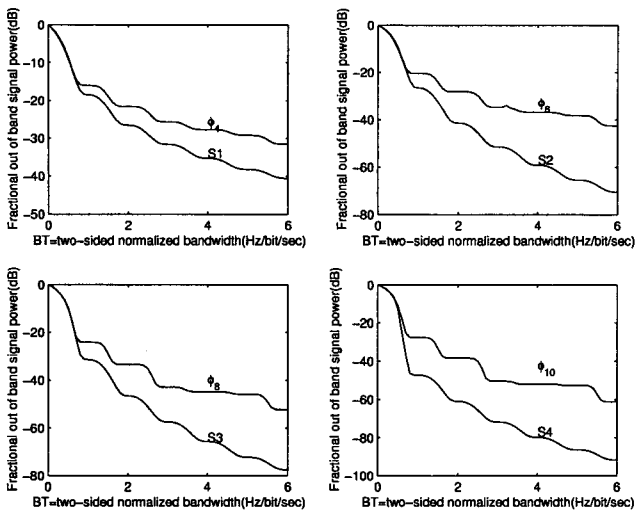


Fig. 4. FOOBP of scaling functions and their approximations.

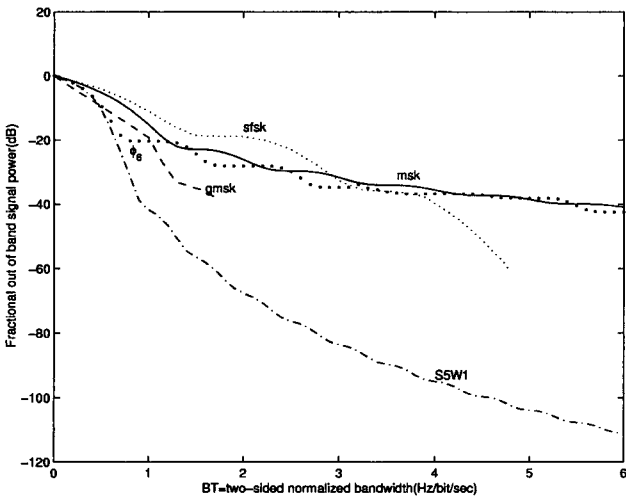


Fig. 5. Comparison between the FOOBP for ϕ_6 , S5W1, MSK, GMSK, and SFSK.

S5 approximating $\phi_6(t/2)$ and W1 approximating $\psi_6(t/2)$. We know that $\phi_6(t/2)$ and $\psi_6(t/2)$ have a combined bandwidth occupancy as $\phi_6(t)$, however, the composite signal S5W1 is more bandwidth efficient than $\phi_6(t)$. Fig. 5 shows the superiority of the FOOBP of S5W1 compared to that of $\phi_6(t)$, MSK, GMSK, and SFSK.

VI. CONCLUSIONS AND DISCUSSIONS

In this paper, application of wavelet and scaling functions as signaling functions for digital communication was put forth. The focus was finding rational approximations of scaling and wavelet functions for efficient hardware implementation. We compared the FOOBP of wavelet functions with some common digital signaling functions and found that particular wavelet functions are significantly more efficient in terms of bandwidth efficiency. A minimax approximation algorithm is applied to find approximate transfer functions at an interval around zero. The circuits built with these rational approximations are pulse-shaping filters that when driven by some special stimulation

functions produce corresponding scaling and wavelet function pulses. We noticed that the correlation penalties were negligible. We then studied the FOOBP of the transfer functions, and found that the transfer functions have even better spectral containment than the wavelet themselves. Compared with partial response continuous-phase modulation (CPM), which also uses pulses with support longer than the signaling interval, wavelet signaling does not require sophisticated detection algorithms such as trellis search.

The tradeoff between residual ISI and the superior spectral containment of these waveforms suggests a new criterion for signal design for digital communications: Design the signal to minimize a combination of ISI and FOOBP. While not claiming that the waveforms here optimally solve this problem, the approximations present a first cut at the solution and suggest that there may be fruitful continued investigations in this area.

REFERENCES

- [1] T. K. Moon, "Wavelets and orthogonal (lattice) spaces," in *Proc. Int. Symp. Inform. Theory*, 1995, p. 250.
- [2] A. R. Lindsey, *Generalized orthogonally multiplexed communication via wavelet packet bases*, Ph.D. thesis, Ohio University, Athens, Ohio, June 1995.
- [3] M. Luise, M. Marselli, and R. Reggiannini, "Clock synchronization for wavelet-based multirate transmissions," *IEEE Trans. Commun.*, vol. 48, pp. 1047-1054, June 2000.
- [4] E. Panayirci, T. Ozugur, and H. Caglar, "Design of optimum Nyquist signals based on generalized sampling theory for data communications," *IEEE Trans. Signal Processing*, vol. 47, pp. 1753-1759, June 1999.
- [5] J. N. Livingston and C.-C. Tung, "Bandwidth efficient signaling using wavelets," *IEEE Trans. Commun.*, vol. 44, pp. 1629-1631, Dec. 1996.
- [6] C. Lo, "Application of wavelet function approximations for bandwidth-efficient digital communication," Master's thesis, Utah State University, Logan, UT, Feb. 1998.
- [7] F. Daneshgaran and M. Mondin, "Bandwidth efficient modulation with wavelets," *Electron. Lett.*, vol. 30, pp. 1200-1202, July 1994.
- [8] R. E. Ziemer and W. H. Tranter, *Principles of communications*. Boston: Houghton Mifflin Company, 3 ed., 1990.
- [9] I. Daubechies, *Ten lectures on wavelets*. Philadelphia, PA: Society for Industrial and Applied Mathematics, 1992.
- [10] A. Ralston and P. Rabinowitz, *A first course in numerical analysis*. New York: McGraw Hill, 2 ed., 1978.
- [11] W. H. Press et al., *Numerical recipes in C*. New York: Cambridge University Press, 2 ed., 1992.



Chet Lo received his B.A. degree in Physics/ Mathematics, M.S. in Mathematics, M.S. in Electrical Engineering, and Ph.D. in Electrical Engineering from Utah State University in 1993, 1997, 1998, and 2001 respectively. He has been awarded the Best International T.A. of The Year and was the winner of the Best Research Paper Competition on Scholar Day at Utah State University. His current research interests include communication in fading multi-path channel and wavelet modulation.



Todd K. Moon received his BS in electrical engineering and mathematics from Brigham Young University, and his masters degree in electrical engineering in 1988. After receiving his PhD in electrical engineering from the University of Utah, he joined the faculty of Utah State University in 1991. His research interests have included wavelet modulation, multi-agent coordination, invariant methods of signal processing, and blind source separation. He is co-author of the book *Mathematical Methods and Algorithms for Signal Processing*.